



ELSEVIER

Contents lists available at ScienceDirect

## Journal of Magnetism and Magnetic Materials

journal homepage: [www.elsevier.com/locate/jmmm](http://www.elsevier.com/locate/jmmm)

## Controlled synthesis and magnetic properties of hard magnetic $\text{Co}_x\text{C}$ ( $x=2, 3$ ) nanocrystals

Yajing Zhang<sup>a</sup>, Girija S. Chaubey<sup>a</sup>, Chuanbing Rong<sup>a</sup>, Yong Ding<sup>b</sup>, Narayan Poudyal<sup>a</sup>, Po-ching Tsai<sup>a</sup>, Qiming Zhang<sup>a</sup>, J. Ping Liu<sup>a,\*</sup>

<sup>a</sup> Department of Physics, University of Texas at Arlington, Arlington, TX 76019, USA

<sup>b</sup> School of Materials Science and Engineering, Georgia Institute of Technology, Atlanta, GA 30332-0245, USA

## ARTICLE INFO

## Article history:

Received 11 November 2010

Received in revised form

9 December 2010

Available online 12 January 2011

## Keywords:

Cobalt carbide

Polyol process

Nanowire

High coercivity

Magnetic property

## ABSTRACT

We report our recent results in synthesis and characterization of cobalt carbide ( $\text{Co}_3\text{C}$  and  $\text{Co}_2\text{C}$ ) nanoparticles and nanowires. The synthesis methods were based on a simple one-pot tetraethylene glycol reduction process. By changing the synthesis parameters, the nanocrystal morphology can be adjusted from nanoparticles with different size to nanowires. The magnetic properties of the nanostructure and their correlation to the crystalline structures and the nanoscale morphology have been investigated theoretically and experimentally. It is revealed that the properties are related to both the crystal structures and the morphology.

© 2011 Elsevier B.V. All rights reserved.

### 1. Introduction

Nanoscale magnetic materials have found wide applications as permanent magnets, magnetic recording media, ferrofluids, and materials hyperthermia [1–8]. Morphology control of the nanoscale materials has always been the research interest because size and shape of the nanoscale materials have direct influence on the applications, especially for ferromagnetic materials.

Cobalt carbide system  $\text{Co}_n\text{C}$  ( $n=1-6$ ) has drawn considerable attention for its interesting structural and physical properties [9,10]. Thin film and bulk materials of the systems have been studied experimentally [11,12]. Theoretical research on the structure of  $\text{Co}_n\text{C}$  ( $n=1-6$ ) clusters has also been reported [13]. However less report can be found in studies of their magnetic properties. In the previous reports,  $\text{Co}_3\text{C}$  was synthesized by mechanical alloying method with precursors of cobalt and carbon powders [14]. Co–C granular films and  $\text{Co}_2\text{C}$  thin film were fabricated via electron beam evaporation and chemical vapor deposition [12,15], respectively. Recently, Harris et al. [16] have reported the cobalt carbide nanoparticles with a coercivity over 3 kOe at room temperature, fabricated by a direct chemical synthesis method. Chemical synthesis of cobalt carbide nanostructures is interesting because of its capability to control the crystal growth in a nanometer scale. In this paper, we report our

recent results in controlled synthesis of cobalt carbide ( $\text{Co}_3\text{C}$  and  $\text{Co}_2\text{C}$ ) nanoparticles and nanowires. The synthesis methods were based on a simple one-pot polyol reduction process assisted with surfactant. By adjusting the category and concentration of the surfactant, shape and size of the cobalt carbide nanocrystals can be controlled, and the magnetic properties of the products can be accordingly tuned.

### 2. Experimental

#### 2.1. Materials

Cobalt nitrate hexahydrate (98%), tetra(ethylene glycol) (TEG, 99%), sodium hydroxide (NaOH, 97%), polyvinylpyrrolidone (PVP, MW~40,000), oleic acid (OA, 90%), absolute ethanol (99.5%)—all the chemicals were commercial products from Sigma-Aldrich Co. and used without further purification.

#### 2.2. Preparation

In a typical procedure, a mixture of 1.25 mmol  $\text{Co}(\text{NO}_3)_2$  and 0.35 g PVP was added to a 125 mL European flask containing 15 mL TEG solvent. The mixture was stirred by a magnetic stirrer for 20 min at room temperature. During this time, 0.05–0.5 g NaOH was dissolved in another 10 mL TEG by heating. After that, 10 mL NaOH solution was injected to the flask. The mixture was first heated to 373 K and held for 30 min to remove water in the

\* Corresponding author.

E-mail address: [pliu@uta.edu](mailto:pliu@uta.edu) (J.P. Liu).

precursors, and then heated to 583 K at a rate of 5 K/min, and refluxed at this temperature for 1–2 h before cooling down to room temperature. During the whole reaction process, Ar gas was purged throughout the container. After the reaction, the obtained product was centrifuged, washed in ethanol for several times, and then dried for characterization.

### 2.3. Characterization

XRD spectra was recorded on a Rigaku Ultima IV diffractometer with a Cu K $\alpha$  X-ray source ( $\lambda=0.15405$  nm). Transmission electron microscopy (TEM) and high-resolution TEM were performed on a HITACHI HF2000 at 200 kV of acceleration voltage and a JEOL4000 with an acceleration voltage of 400 kV. Samples for TEM analysis were prepared by depositing nanoparticle solutions onto an amorphous carbon-coated copper grid. The magnetic property measurements were carried out by using a superconducting quantum interference device (SQUID) magnetometer with magnetic fields up to 1.5 T. The temperature-dependent magnetic property was measured by a quantum design physical property measurement system (PPMS) from 300 to 900 K with a magnetic field of 1.5 T.

## 3. Results and discussion

### 3.1. Cobalt carbides synthesis

The procedure and conditions described in the experimental section were found to be optimal for the production of cobalt nanoparticles. Fig. 1 shows the XRD pattern of the as-synthesized cobalt carbide nanoparticles, which can be indexed to the JCPDS reference powder diffraction files Co<sub>2</sub>C (72–1371) with space group Pm $\bar{3}n$  ( $a=2.90$  Å,  $b=4.45$  Å and  $c=4.37$  Å) and Co<sub>3</sub>C (89–2866) with space group Pnma ( $a=5.08$  Å,  $b=6.73$  Å and  $c=4.52$  Å). This XRD result indicates that the product is a mixture of two phases of Co<sub>2</sub>C and Co<sub>3</sub>C. The average grain size of the cobalt carbides is 14 ( $\pm 2$ ) nm as determined by Scherrer formula from XRD data.

The amount of the surfactant of PVP was found to be an important parameter in determining the size of the cobalt carbide nanoparticles. Typical TEM pictures of the particles prepared with different amount of PVP (ranging from 0 to 0.5 g) are shown in Fig. 2. With increase in the amount of the surfactant of PVP, the

size of the as-synthesized cobalt carbide nanoparticles decreases, as shown in Fig. 2(a)–(c). For example, without PVP, the cobalt carbide spheres with an average diameter of 1000 nm were obtained (Fig. 2(a)), while with 0.35 g PVP, the size decreased to 20 nm. However, if the amount of PVP is further increased to 0.5 g, the size of the nanoparticles will not decrease anymore, but chains particles several micrometer long are formed with a chain average diameter of about 200 nm.

It is known that the surfactant plays two important roles in controlling growth of the nanocrystals: (1) absorption on the surface of the as-prepared primary building blocks, which prevents primary building blocks from entropy-driven random aggregation [17–20] and (2) anisotropic interactions between the surfactant and the different facets of the nanocrystals, which controls the formation of differently shaped nanocrystals [21–23]. The dependence of the size on PVP concentration during the formation of cobalt carbide is related to the adsorption of PVP on the nanoparticle surface.

It has also been found from our study that the shape of the cobalt carbide can be controlled by changing the surfactant. For example, if oleic acid (OA) is used as the surfactant instead of PVP, cobalt carbide nanowires can be obtained, as shown in Fig. 3. Fig. 3(a) shows TEM image of the cobalt carbide nanowires having a diameter of about 5 nm with lengths of about 80 nm. It should be noted that there was a small amount of nanoparticles having a diameter of about 10 nm with very weak contrast observed in the TEM image together with the nanowires. Fig. 3(b) is the high-resolution TEM (HRTEM) image recorded on an individual nanowire, and the marked lattice space is 0.25 nm, which has a good match with the (1 0 1) face of Co<sub>2</sub>C structure. The fast Fourier transform (FFT) was obtained from the HRTEM image that provides further insight into the structure and the preferred growth directions of the nanowires, as shown in the right top corner in Fig. 3(b), which can be indexed to the Co<sub>2</sub>C structure with an orientation of [0 1 0] zone axis. Fig. 3(c) is an HRTEM image of nanoparticles with a weak contrast in Fig. 3(a). Similarly, the marked planar distance of 0.21 nm is consistent with the ( $\bar{2}$  1 1) lattice space of Co<sub>3</sub>C structure, and the FFT (shown in the bottom corner of Fig. 3(c)) can be indexed to the Co<sub>3</sub>C structure with an orientation of [2 1 3] zone axis. The result confirms that the product is a mixture of Co<sub>3</sub>C and Co<sub>2</sub>C. It is believed that the anisotropic interaction between oleic acid and the different facets of the nanoparticles should be the key point for the formation of one-dimensional nanowires [24,25]. Our results show that the size and the shape of the cobalt carbide nanocrystals can be controlled by simply adjusting the amount of the surfactant and by changing the types of surfactants.

In this polyol reduction process, TEG was used not only as a solvent but also as a reducing agent [26]. In order to know where the carbon to form the cobalt carbides has come from, a comparison experiment was carried out. Without any surfactant, mixtures of Co<sub>2</sub>C and Co<sub>3</sub>C were still obtained as the product, while keeping other reaction parameters unchanged, indicating that the carbon in the cobalt carbide comes from the solvent of TEG.

To investigate the growth mechanism of the cobalt carbide nanocrystals, systematic time-dependent experiments illustrating the evolution of the structure were also carried out at various growth stages of the reaction process. Based on our experimental results and the results reported elsewhere [27,28], we propose the formation mechanism of the cobalt carbide nanocrystals as shown in the schematic in Fig. 4. We assume that the formation of cobalt carbide nanocrystals takes place in three steps (Fig. 4(a)): (1) the cobalt nanoparticles are reduced by the solvent TEG; (2) the cobalt nanoparticles catalyze TEG to generate active carbon atoms; (3) the active carbon atoms diffuse into the cobalt nanoparticles gradually to form the cobalt carbide nanoparticles.

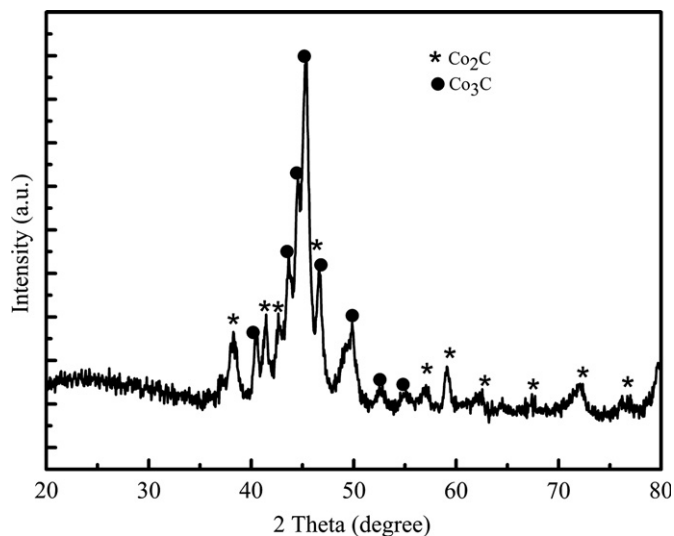
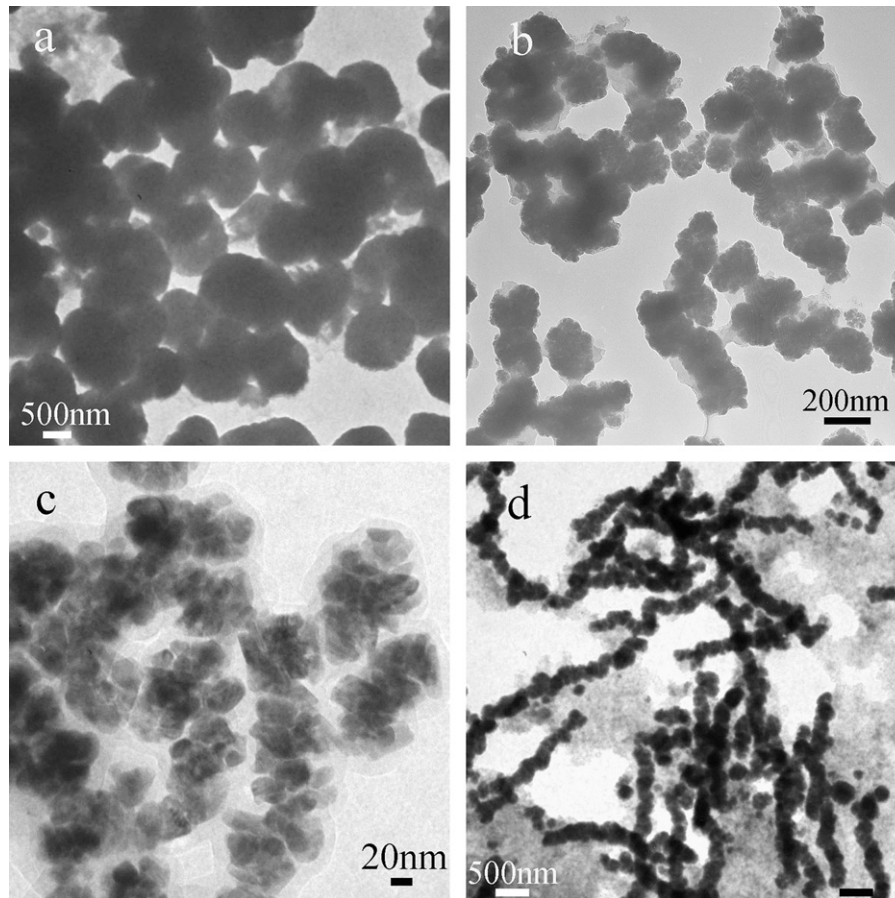
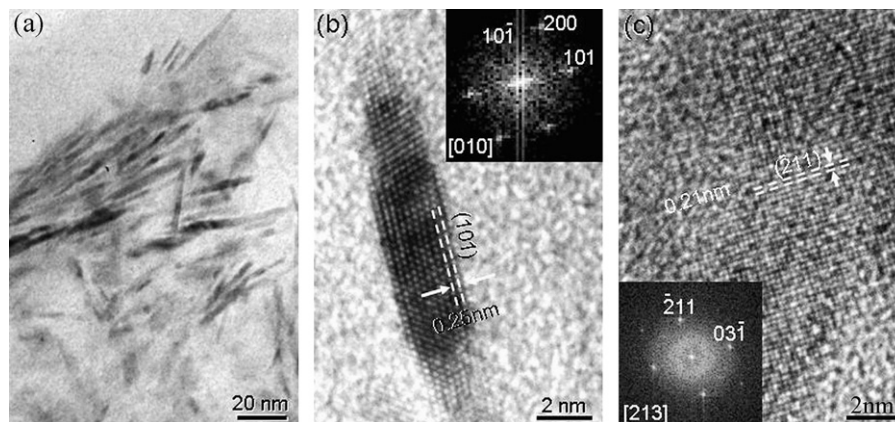


Fig. 1. XRD pattern of the as-prepared product by reduction of cobalt nitrate in a 0.15 M NaOH solution in tetraethylene glycol.



**Fig. 2.** TEM images of cobalt carbide nanoparticles obtained with different amount of PVP in TEG solution: (a) 0 g; (b) 0.15 g; (c) 0.35 g; and (d) 0.5 g.



**Fig. 3.** (a) TEM image of the cobalt carbide nanowires obtained with surfactant of OA; (b) HRTEM image of an individual nanowire shown in (a) (insert: the FFT from a part of the nanowire); and (c) HRTEM image of an individual nanoparticle shown in (a) (insert: the FFT from a part of the nanoparticle).

A similar formation mechanism is proposed for the cobalt carbide nanowires, as plotted in Fig. 4(b). Firstly, the cobalt nanoparticles are reduced during the reaction process. Secondly, the as-reduced nanoparticles grow along a certain direction to form nanowires in the presence of the surfactant of OA. Thirdly, the cobalt nanowires also catalyze the solvent producing active carbon atoms. Lastly, the activated carbon atoms diffuse into the cobalt nanowires and therefore form the cobalt carbide nanowires. High resolution TEM observations of samples are collected at different stages of reactions to find the core/shell structure. However, possibly because of the fast interdiffusion process during the nanoparticle growth, the clear core/shell structure was not observed.

By this polyol reduction process, one-dimensional chain-like nickel carbide nanocrystals were also synthesized. It is believed that this simple method can be extended to synthesize other nanostructured transition metal carbides.

### 3.2. Magnetic properties

According to an earlier electron diffraction study by Nagakura [29], there is a relationship between the crystal structures of hcp  $\alpha$ -Co and the cobalt carbides. The lattice relation is that the (0 0 1) plane of  $\text{Co}_2\text{C}$  is parallel to the (0 0 1) plane of  $\alpha$ -Co, and the

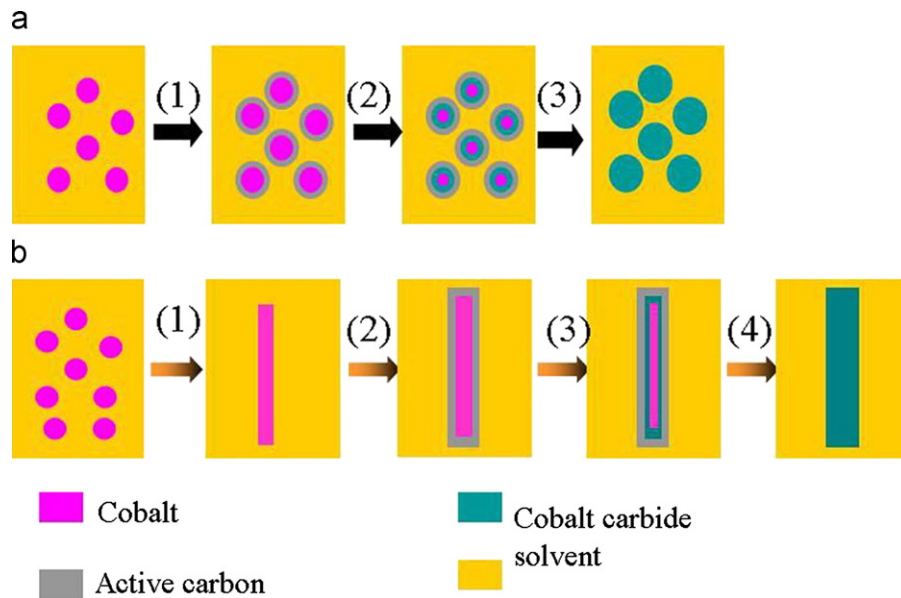


Fig. 4. Illustration of the formation mechanism of the cobalt carbides (a) nanoparticles and (b) nanowires.

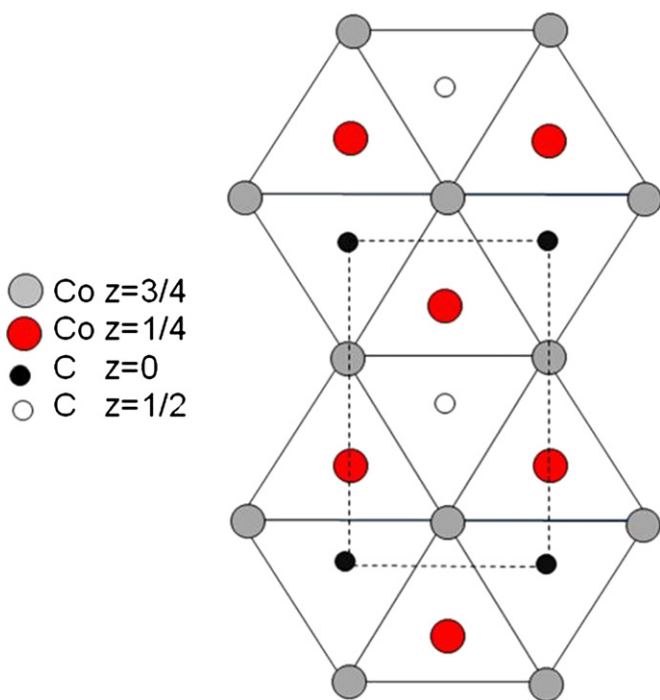
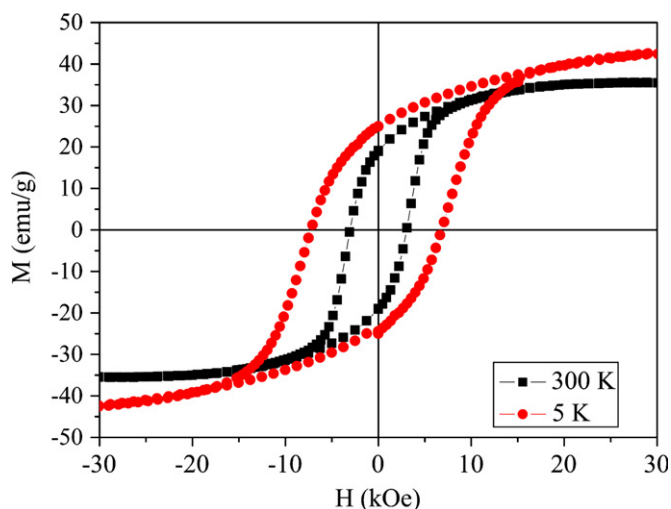


Fig. 5. A schematic of  $\text{Co}_2\text{C}$  prime cell inside the  $\alpha\text{-Co}$  lattice with  $[001]$  pointing outside of the paper. The big circles are Co atoms while the small circles are C atoms. The real lines form the hcp lattice of  $\alpha\text{-Co}$  while the dashed lines form the orthorhombic lattice of  $\text{Co}_2\text{C}$ . The real structure may have a slight relaxation from it.

$[100]$  direction of  $\text{Co}_2\text{C}$  is parallel to the  $[100]$  direction of  $\alpha\text{-Co}$ , as shown in Fig. 5. Obviously,  $\text{Co}_2\text{C}$  is an interstitial compound after the diffusion of carbon atoms into the cobalt lattices. On the other hand,  $\text{Co}_3\text{C}$  has a  $\text{Fe}_3\text{C}$  structure [30]. There are 4 molecules in its orthorhombic prime cell in the  $\text{Co}_3\text{C}$  structure, with two types of Co atoms. The lattice relation with  $\alpha\text{-Co}$  is not as simple as that of  $\text{Co}_2\text{C}$ . According to Nagakura, the  $[1\bar{2}1]$  plane of  $\text{Co}_3\text{C}$  is parallel to the  $(101)$  plane of  $\alpha\text{-Co}$ , and the  $[111]$  direction of  $\text{Co}_3\text{C}$  is parallel to the  $[0\bar{1}0]$  direction of  $\alpha\text{-Co}$  [29].

Based on the crystal structures, first-principles DFT-based calculations have been conducted on the cobalt carbides. The PAW method with GGA-PBE potentials built in VASP software package has been used [31]. The optimized structures are in good agreement with our XRD measurements (within  $\sim 2\%$ ). One advantage of the theoretical study is that  $\text{Co}_2\text{C}$  and  $\text{Co}_3\text{C}$  can be studied individually while it is difficult to separate them in the experiments. The calculations show that the two phases have different magnetic structures. The magnetization of  $\text{Co}_3\text{C}$  is still substantial, though lower than that of  $\alpha\text{-Co}$ , with a value of about  $1.02 \mu_B$  per Co atom. On the other hand, the magnetization of  $\text{Co}_2\text{C}$  is almost vanished, about  $0.04 \mu_B$  per Co atom. This indicates that the magnetic property of the nanostructures obtained in the present experiment is contributed mainly by  $\text{Co}_3\text{C}$ . In  $\text{Co}_2\text{C}$ , each Co atom has 3 carbon atoms as the first nearest neighbor (n.n.), with a bond length of  $\sim 1.90 \text{ \AA}$ . But in  $\text{Co}_3\text{C}$ , there are two types of Co atoms, 4 Co(I) and 8 Co(II), in a prime cell. The Co(I) has 2 carbon atoms in its first n.n., with a bond length of  $\sim 1.92 \text{ \AA}$ . The Co(II) has 2C atoms in its first n.n., with a bond length of  $\sim 1.97 \text{ \AA}$ , and another C atom in its second n.n. with a bond length of  $2.38 \text{ \AA}$ . The Co–C bonding may weaken the metallic bond, and hence the exchange interaction among Co atoms. The crystal structure of  $\text{Co}_3\text{C}$  has a much lower symmetry than that of  $\alpha\text{-Co}$ . This will enhance the magnetocrystalline anisotropy and, in turn, the coercivity of the material. The calculation of the magnetocrystalline anisotropy is undergoing and will be published separately.

The coercivity is an important parameter of magnetic nanomaterials which not only relates to the magnetic anisotropy, including magnetocrystalline anisotropy, exchange anisotropy, and shape anisotropy, but also relates to the size and preparation conditions for the magnetic nanocrystals [32,33]. Our study shows that the coercivity values of cobalt carbides can be controlled by simply adjusting synthesis parameters and therefore adjusting the morphology and composition of the obtained products. As an example, it was measured that the cobalt carbide nanoparticles of 1000, 200, and 20 nm size (shown in Fig. 2) have their coercivity values of 0.6, 1.7, and 3.1 kOe, respectively, indicating that the coercivity values increase with decreasing particle size. It is also observed that although the samples shown in Fig. 2(b) and (d) have the same average diameter, the coercivity



**Fig. 6.** Hysteresis loops of cobalt carbide nanoparticles with diameter of 20 nm at (a) 300 K (square spot, black line) and (b) 5 K (circle spot, red line). (For interpretation of the references to color in this figure legend, the reader is referred to the web version of this article.)

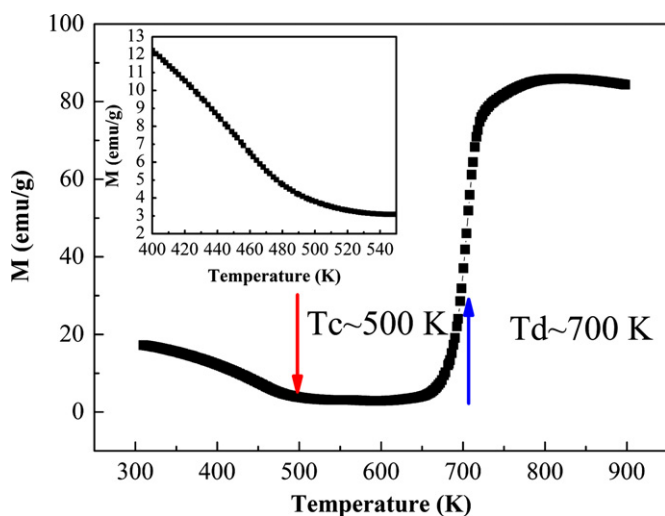
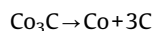
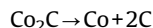


**Fig. 7.** Temperature dependent magnetization for the 20 nm cobalt carbide nanoparticles with an applied magnetic field of 1.5 T (inset is the local part of the curve).

value (2 kOe) of the sample shown in Fig. 2(d) is higher than that of the sample shown in Fig. 2(b), implying that the one-dimensional self-assembled chain-like nanocrystals have higher magnetic anisotropy [34]. The chain-like structure has a length to diameter ratio of about 25, which contributes to the shape anisotropy of the nanostructures.

Fig. 6 shows magnetic hysteresis loops of as-synthesized 20 nm cobalt carbide nanoparticles at 300 and 5 K. This figure reveals that the magnetizations at both room and low temperatures are saturated under the field of 30 kOe. The cobalt carbide nanoparticles have coercivity values of 3.1 and 7.3 kOe with saturation magnetizations of 35.5 and 42.8 emu/g, respectively. Fig. 7 shows the temperature dependent magnetization curve for the 20 nm cobalt carbide nanoparticles from 300 to 900 K under a magnetic field of 1.5 T. The mean heating rate is 10 K/min. Fig. 7 infers the nanoparticles have a Curie temperature near 500 K. It can be seen that there is a dramatic increase in magnetization at about 700 K, which is due to the thermal decomposition of the cobalt carbide nanoparticles at high temperatures. To verify this

conjecture, the cobalt carbide nanoparticles were annealed in vacuum at 773 K for 30 min, then the XRD result showed that the obtained sample after the annealing was the mixture of cobalt and graphite. This thermal process can be expressed as the following equations [14]:



The fact that cobalt carbide compounds decompose at high temperature has also been reported by other researchers. Tokumitsu [14] found that the  $\text{Co}_3\text{C}$  prepared by mechanical alloying method has a phase decomposition at temperatures between 468 and 524 °C (determined by DSC), and the decomposition temperature varied with heating rate; the decomposition temperature becomes lower with decreasing heating rate. This thermal instability may provide an alternative method for fabrication of cobalt nanoparticles and granular films. Indeed, Jiang et al. [15] obtained cobalt nanostructures in carbon films via decomposition of  $\text{Co}_2\text{C}$  films.

#### 4. Summary

In summary, a facile polyol reduction procedure has been developed for preparation of cobalt carbide nanoparticles and nanowires. The use of the surfactant is the key to control the morphology of the nanocrystals. The formation mechanism of the nanoparticles and nanowires has been discussed. The crystal structure and their magnetic properties are investigated via both experimental and theoretical studies. Correlation between the magnetic coercivity and the morphology has been revealed. The highest coercivity of the obtained cobalt nanocrystals is 3.1 kOe at room temperature. This polyol reduction may be extended to the preparation of nanocrystals of other pure transition metals and their carbides.

#### Acknowledgment

This work has been supported in part by the US Office of Naval Research/MURI project under Grant N00014-05-1-049, US DoD/DARPA/ARO under Grant W911NF-08-1-0249, and by the University of Texas-Arlington.

#### References

- [1] S.H. Sun, C.B. Murray, D. Weller, L. Folks, A. Moser, *Science* 287 (2000) 1989.
- [2] S.D. Bader, *Rev. Mod. Phys.* 78 (2006) 1.
- [3] X. Peng, L. Manna, W. Yang, J. Wickham, E. Scher, A. Kadavanich, A.P. Alivisatos, *Nature* 404 (2000) 59.
- [4] S. Odenbach, *J. Phys.: Condens. Matter* 16 (2004) R1135.
- [5] S. Momet, S. Vasseur, F. Grasset, E. Duguet, *J. Mater. Chem.* 14 (2004) 2161.
- [6] D. Ung, Y. Soumare, N. Chakroune, G. Viau, M.-J. Vaulay, V. Richard, F. Fiévet, *Chem. Mater.* 19 (2007) 2084.
- [7] B. Viswanath, P. Kundu, A. Halder, N. Ravishankar, *J. Phys. Chem. C* 113 (2009) 16866.
- [8] R.C. O'Handley, *Modern Magnetic Materials: Principles and Applications*, Wiley, New York, 1999, p. 469.
- [9] M.E. McHenry, S.A. Majetich, J.O. Artman, M. DeGraef, S.W. Staley, *Phys. Rev. B* 49 (1994) 11358.
- [10] Z.D. Zhang, J.L. Yu, J.G. Zheng, I. Skorvanek, J. Kovac, X.L. Dong, Z.J. Li, S.R. Jin, H.C. Yang, Z.J. Guo, W. Liu, X.G. Zhao, *Phys. Rev. B* 64 (2001) 024404.
- [11] Y.H. Lee, Y.S. Huang, J.F. Min, G.M. Wu, L. Horn, *J. Magn. Magn. Mater.* 310 (2007) 913.
- [12] P.A. Premkumar, A. Turchanin, N. Bahlawane, *Chem. Mater.* 19 (2007) 6206.
- [13] Z.X. Zhang, B.B. Cao, H.M. Duan, *J. Mol. Struct.: THEOCHEM* 863 (2008) 22.
- [14] K. Tokumitsu, *Mater. Sci. Forum* 127 (1997) 235–238.
- [15] J.C. Jiang, X.Y. Nie, E.I. Meletis, *Int. J. Nanomanuf.* 2 (2008) 16.
- [16] V.G. Harris, Y. Chen, A. Yang, S. Yoon, Z. Chen, A.L. Geiler, J. Gao, C.N. Chinnasamy, L.H. Lewis, C. Vittorial, E.E. Carpenter, K.J. Carroll, R. Goswami, M.A. Willard, L. Kurihara, M. Gjoka, O. Kalogirou, *J. Phys. D: Appl. Phys.* 43 (2010) 165003.

- [17] Y.G. Sun, B. Gates, B. Mayers, Y.N. Xia, *Nano Lett.* 2 (2002) 165.  
[18] J.W. Wang, X. Wang, Q. Peng, Y.D. Li, *Inorg. Chem.* 43 (2004) 7552.  
[19] A. Umar, M. Oyama, *Cryst. Growth Des.* 6 (2006) 818.  
[20] Z.P. Zhang, X.Q. Shao, H.D. Yu, Y.B. Wang, M.Y. Han, *Chem. Mater.* 17 (2005) 332.  
[21] Q. Xie, Y.T. Qian, S.Y. Zhang, S.Q. Fu, W.C. Yu, *Eur. J. Inorg. Chem.* 12 (2006) 2454.  
[22] L. Gou, C.J. Murphy, *Chem. Mater.* 17 (2005) 3668.  
[23] C. Wang, Y. Hou, J. Kim, S. Sun, *Angew. Chem. Int. Ed.* 46 (2007) 6333.  
[24] M. Chen, J. Kim, J.P. Liu, H. Fan, S. Sun, *J. Am. Chem. Soc.* 128 (2006) 7132.  
[25] Y. Wang, H. Yang, *J. Am. Chem. Soc.* 127 (2005) 5316.  
[26] G. Viau, F. Fiévet-Vincent, F. Fiévet, *Solid State Ionics* 84 (1996) 259.  
[27] W. Zhou, K. Zheng, L. He, R.M. Wang, L. Guo, C.P. Chen, X.D. Han, Z. Zhang, *Nano Lett.* 8 (2008) 1147.  
[28] Y.H. Leng, H.Y. Shao, Y.T. Wang, M. Suzuki, X.G. Li, *J. Nanosci. Nanotech.* 6 (2006) 221.  
[29] S. Nagakura, *J. Phys. Soc. Jpn.* 16 (1961) 1213.  
[30] R.W.G. Wychoff, *Crystal Structures*, vol. 2, Wiley-Interscience, New York, 1960.  
[31] G. Kresse, D. Joubert, *Phys. Rev. B* 59 (1999) 1758.  
[32] M. Yu, Y. Liu, D.J. Sellmyer, *J. Appl. Phys.* 87 (2000) 6959.  
[33] A. Fert, L. Piraux, *J. Magn. Magn. Mater.* 200 (1999) 338.  
[34] I.S. Jacobs, C.P. Bean, *Phys. Rev.* 100 (1955) 1060.